Nanoscale

Accepted Manuscript

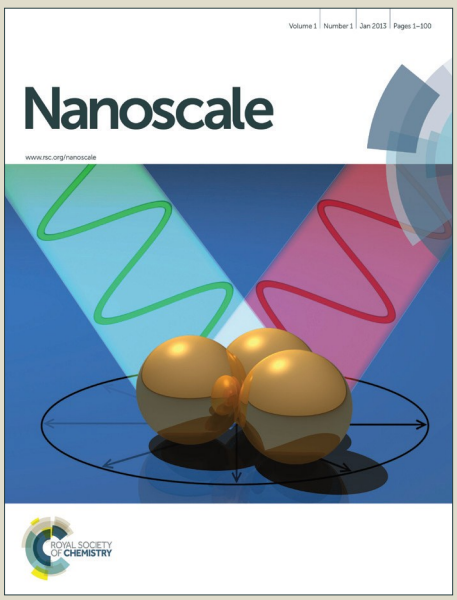

ROYAL SOCIETY OF CHEMISTRY

www.rsc.org/nanoscale

Journal Name

COMMUNICATION

Inclusion of Cu Nano-cluster 1D Arrays inside a C_3-Symmetric Artificial Oligopeptide via Co-assembly

Received 00th January 20xx,
Accepted 00th January 20xx

DOI: 10.1039/x0xx00000x

www.rsc.org/

Ruiying Gong,[a] Fei Li,[a] Chunpeng Yang,[a] Xiaobo Wan [a]*

A peptide sequence N_3-GVGV-OMe (G: glycine; V: valine) was attached to a benzene 1,3,5-tricarboxamide (BTA) derivative via "click chemistry" to afford a C_3-symmetric artificial oligopeptide. The key feature of this oligopeptide is that the binding sites (triazole groups formed by click reaction) are located at the center, while the three oligopeptide arms with strong tendency to assemble are located around them, which provides inner space to accommodate nanoparticles via self-assembly. The inclusion of Cu nanoclusters and the formation of one-dimensional (1D) arrays inside the nanofibers of the C_3-symmetric artificial oligopeptide assembly were observed, which is quite different from the commonly observed nanoparticle growth on the surface of the pre-assembled oligopeptide nanofibers via the coordination sites located outside. Our finding provides an instructive concept for the design of other stable organic-inorganic hybrids 1D arrays with the inorganic nanoparticles inside.

The synthesis and assembly of one-dimensional (1D) metallic nanoparticles assisted by bio-organic molecules are interesting topics in nano science. Especially, protein or peptide directed metallic nanoparticle assembly has attracted much attention in the past decades due to the versatility of peptide pool, the mild preparation conditions, the controllable sizes and shapes of the resultant nano-structures, and the specific functions resulting from the hybridization of metallic and organic functionalities, which were summarized in recent reviews.[1-5] In many cases, the metallic nanoparticles are immobilized on the surface of assembled peptide nanofibers, via specific interactions such as ligand-metal complexation and electrostatic attraction. For instance, Matsui and co-workers reported Cu nano-crystal growth on a bolaamphiphile peptide nanotube, the surface of which is pre-modified with a sequenced histidine-rich peptide.[6] The interaction between the histidine moiety and Cu provided the driving force for the assembly. Porchan et al reported 1D assembly of negatively charged Au nanoparticles onto the surface of 17H6 nanofibrils by neutralizing the positively-charged histidine moiety on the peptide.[7] This concept was widely used in the preparation of other 1D metallic or inorganic nanoparticles assemblies.[8-18] On the other hand, the inclusion of metallic nanoparticles inside proteins or peptides to form 1D structure was realized mainly through capillary effects but was scarcely reported. Reches and Gazit reported the in-situ reduction of Ag^+ ions filled inside diphenylalanine (Di-Phe) nanotubes to form Ag nanowires.[19] The incorporation of Fe_3O_4 nanoparticles inside a bolaamphiphile peptide at low concentration has also been reported.[9] Due to the non-specific nature of capillary effects, the nanowire/nanoparticle growth inside the tube may coexist with the nanoparticles growth on the surface in the presence of other interactions.[20-22] The reports on inclusion of metal nanoparticles through specific interaction inside the peptides are rare. One recent example is to use electrostatic attraction to immobilize $AuCl_4^-$ inside a peptide, which was further reduced in situ to give Au nanoparticles inside to form nanoribbons.[23] Here we wish to report a simultaneous inclusion of Cu nano-clusters inside a C_3-symmetric artificial oligopeptide assembly through ligand-metal complexation to form 1D arrays. The key feature of this oligopeptides is that the binding sites are located at the center, while the three oligopeptide arms with strong tendency to assemble are located around, which provides space to accommodate nanoparticles via self-assembly. This concept might be instructive for the design of other stable novel 1D nanoparticle arrays.

The C_3-symmetric artificial oligopeptide was constructed from two components by click chemistry: one is an oligopeptide with a terminal azide group which has the strong tendency to form β-sheet, namely N_3-GVGV-OMe,[24] and the other one is a benzene 1,3,5-tricarboxamide (BTA) derivative with a terminal alkynyl group. BTA is a versatile building block for self-

CAS Key Laboratory of Bio-based Materials, Qingdao Institute of Bioenergy and Bioprocess Technology, Chinese Academy of Sciences, 189 Songling Road, Qingdao, Shandong Province, 266101, P. R. China
Email: wanxb@qibebt.ac.cn.

Electronic Supplementary Information (ESI) available: Detailed synthesis, gel preparation, general methods for characte-rization, and the characterisation of BTA-C_3-GVGVOMe assembly including or not including Cu nano-cluster arrays. This material is available free of charge via seeing DOI: 10.1039/x0xx00000x.

assembly[25] and was used to form chiral nano-assemblies for asymmetric catalysis recently.[26] The growth of Au nanoparticles on the surface of such assemblies was also reported.[27] BTA-oligopeptides conjugate was firstly reported by Matsuura et al and the formation of nanofibers consisting of β-sheets was observed.[28] The click reaction between N_3-GVGV-OMe **1** and N, N', N''-tris-propargyl benzene-1,3,5-tricarbox-amide **2** underwent smoothly to give the C_3-symmetric artificial oligopeptide **3** (BTA-C_3-GVGVOMe) in excellent yield and also installed three triazole groups between the BTA core and the oligopeptide arms, as shown in Scheme 1. Details of the synthesis and characterization are reported in the Supporting Information. The analytical and spectroscopic data for oligopeptide **3** are fully consistent with its molecular structure.

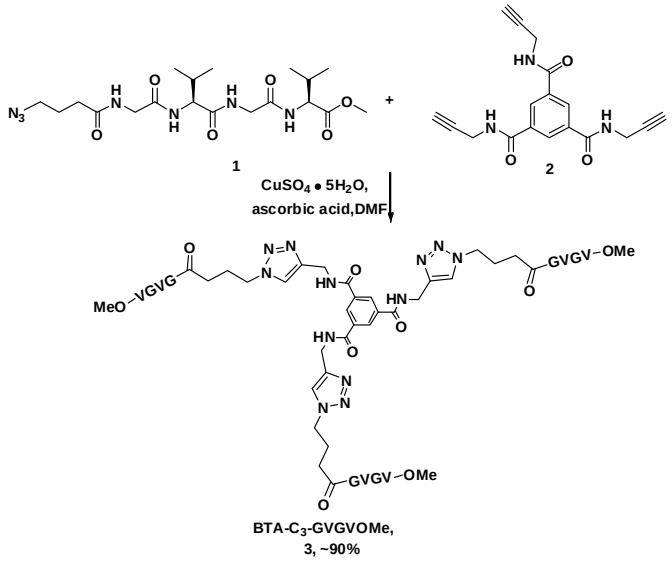

Scheme 1. Synthesis route of BTA-C_3-GVGVOMe 3.

BTA-C_3-GVGVOMe showed good solubility in hot DMF/MeOH, and gradually formed an organogel during storage. The assembly of purified BTA-C_3-GVGVOMe is conducted through a colloidal self-assembly method. In a typical experiment, oligopeptide **3** (0.01g, 0.006 mmol) was dissolved in DMF/MeOH (120 μL, 5:1 volume ratio) at 65°C and then incubated at 36°C for 30 days to form stable gel. Scanning electron microscope (SEM) images show that the purified artificial peptide assembles into nanofibers up to several micrometers long with widths ranging from 20 to 100 nm under low scanning voltage (3 KV) (Figure S1).The transmission electron microscopy (TEM) images the purified artificial peptide 3 (Figure 1a and Figure S2) also confirmed the formation of these nanofibers.

Surprisingly, if BTA-C3-GVGVOMe was not thoroughly purified (there were some residual catalysts (CuSO4•5H2O) and ascorbic acid), the formation of aligned nanoparticles along the axis of the nanofibers (Figure 1b) was observed under the same preparation conditions. Furthermore, different from many previous reports, these nanoparticles seem to be located inside the nanofibers, since the edge of the nanofibers is smooth and no growth of the nano-particles on the edge was observed (as indicated by the arrows in Figure 1c).The difference of the two types of alignments is schematic denoted in Figure 1d. The size of the nanoparticles ranges from 5 to [illegible] nm. We reasoned that the nanoparticles should be Cu(0) clusters, since Cu(II) could be reduced to Cu(0) in the presence of ascorbic acid. Indeed, ascorbic acid is a mild reducing reagent in the preparation of many metallic nano-materials including Cu(0).[29] High-resolution TEM image (the insert in Figure 1 c, full image in Figure S3) clearly shows that the nanoparticles inside the artificial oligopeptide are crystalline, with a d space around 0.18 nm, which corresponds to (200) plane of Cu(0). X-ray photoelectron spectroscopy (XPS) of the xerogel showed two peaks at 954.7 eV and 932.6 eV, which also correspond to Cu2p1/2 and Cu2p3/2 of Cu(0), respectively (Figure S4).

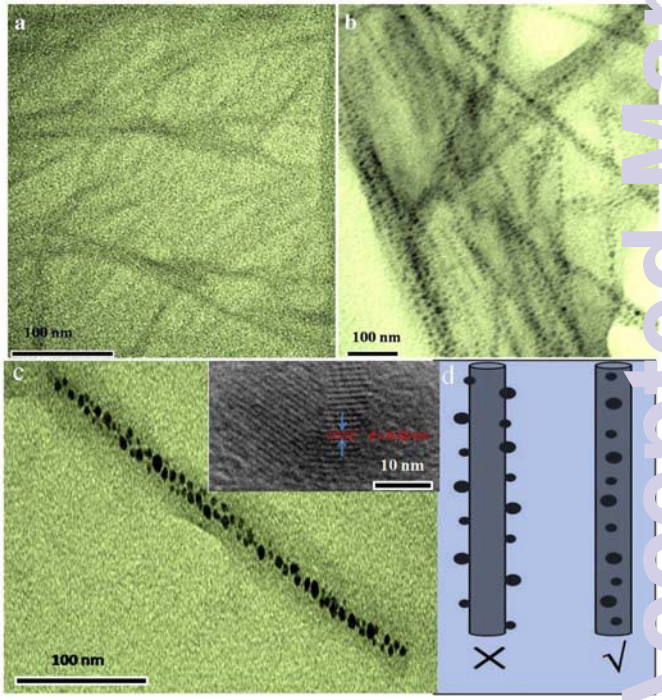

Figure 1. TEM images of the assembly morphology of gel@ BTA-C3-GVGVOMe (a) and gel@ BTA-C3-GVGVOMe &Cu (b). (c) Enlarged TEM image of one-dimensional Cu nanoclusters array. (d) Schematic diagram of Cu nanoclusters aligned along the nanostructured gel fibers.

The role of ascorbic acid in the formation of Cu(0) 1D arrays inside the C_3-symmetric oligopeptide **3** was confirmed in a control experiment. If the purified oligopeptide **3** was incubated just with $CuSO_4•5H_2O$ at the same conditions for gel formation, no Cu(0) nano particle formation was observed. This is understandable since the oligopeptide itself does not have the reductive center to reduce Cu (II). On the other hand, when the purified oligopeptide **3** was incubated with $CuSO_4•5H_2O$ and ascorbic acid, the formation of the Cu(0) 1D arrays inside the nanofibers was re-observed. Furthermore, the amount of Cu(0) incorporated into the oligopep-tide nanofibers could be modulated by changing the molar feeding ratio of Cu(II) toward oligopeptide. Three feeding ratios (0.6:1; 1.2:1; 2.4:1) were set and the TEM images of the obtained Cu(0)-oligopeptide nanofibers are listed in Figure 2. When 0.6 equiv. of Cu(II) was incubated with oligopeptide in the presence of ascorbic acid (Figure 2a), the nanofibers with Cu(0)

nanoparticles inside are very similar to that obtained from not well-purified oligopeptides. When the molar ratio of Cu(II) was increased to 1.2 equiv or higher, those nanofibers tended to aggregate into larger but shorter bundles.

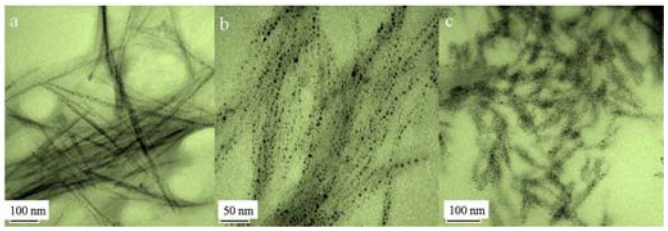

Figure 2. TEM images of the assembly morphology of gel@ BTA-C_3-GVGVOMe &Cu at different Cu: oligopeptide molar ratio. (a): 0.6:1; (b): 1.2:1, (c): 2.4:1. In each case, the molar content of the ascorbic acid is twice as much as that of $CuSO_4 \bullet 5H_2O$.

The formation of Cu nanoparticles arrays inside the oligopeptide fiber was further confirmed by SEM at elevated voltage. In low-voltage (3 kV) SEM technique, electrons interact with the surface of the specimen, and the corresponding images are more sensitive to the chemical and topographic form of the surface. In conventional voltage region (10 to 30 kV), SEM images reflect more about the structure of the bulk.[30] Furthermore, due to the heavy-atom effects, Cu should have stronger signal in SEM than peptides. The comparison of the SEM images of organogel obtained from BTA-C_3-GVGVOMe and BTA-C_3-GVGVOMe &Cu (obtained at 2.4 equiv. Cu(II) feeding ratio) at different scanning voltages is shown in Figure 3. At 3 kV scanning voltage, both gels showed similar SEM images (nanofibers with similar brightness, Figure 3a and 3c), indicating that the surface of both nanofibers might be composed from similar elements. At 20 kV scanning voltage, the image of nanofiber of BTA-C_3-GVGVOMe (Fig. 3b) did not show much difference from that obtained at 3 kV voltage, inferring that the elements (C, N, O atoms from the oligopeptides) in the bulk showed little difference from those in the surfaces of the nanofibers. On the other hand, the images of BTA-C_3-GVGVOMe &Cu nanofibers obtained at 20 kV exhibit many dazzling nanofibers with enhanced brightness (Figure 3d and Figure S5a-5d) , which are assigned to the Cu(0) arrays inside the oligopeptide nanofibers. Two enlarged images of the dazzling nanofibers are shown in the inset of Figure 3d and Figure S5d, and the smooth edge of these nanofibers further implied that no Cu nanoparticles were immobilized on the surface.

The inclusion of Cu(0) nanoparticles inside the three-armed peptides makes those nanoparticles stable to long-term storage. Figure S6 showed the image of the assembled nano-fibers which have been stored on the shelf for 2 years. No aggregation of these nanoparticles was observed.

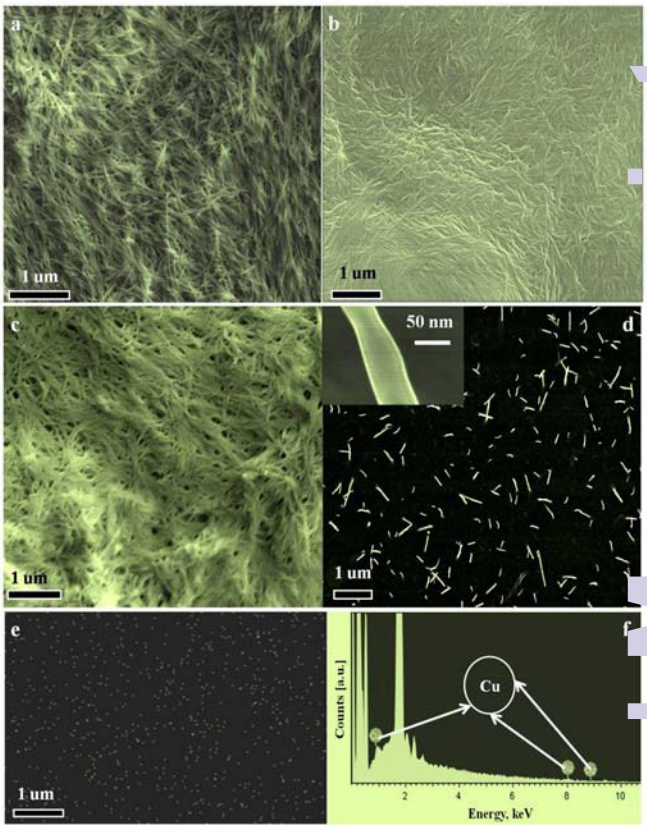

Figure 3. SEM images of the assembly morphology of gel@ BTA-C_3-GVGVOMe (a: at 3 KV scanning voltage) and (b: at 20 KV scanning voltage) (c) and (d) are the SEM images of the assembly morphology of gel@ BTA-C_3-GVGVOMe &Cu obtained at 2.4 equiv. of Cu(II) at 3 KV scanning voltage and at 20 KV scanning voltage, respectively. (e) The elemental map for Cu in the image (d). (f) The energy dispersive spectrometer (EDS) of Cu in the image (d).

Based on these results, the mechanism of self-assembly of Cu(0)-oligopeptides nanofibers was proposed, and is shown in Figure 4. As stated earlier, the most important feature of BTA-C_3-GVGVOMe is that triazole groups located inside acts as the coordination center and the oligopeptide with strong tendency for self-assembly at the periphery acts as the assembly center. The complexation of triazole group with Cu(II) has been well documented,[31] and therefore it is reasonable to postulate that the Cu(0) nanoparticles were formed either through the formation of Cu(II)-triazole complex during the incubation period followed by the reduction by ascorbic acid, or the reduction first then followed by coordination, or these two processes occurred simultaneously. To prove this, a control experiment was carried out to co-assemble the pre-synthesized Cu nannocluster with the purified oligopeptide. Cu nannocluster was prepared by mixing ascorbic acid and $CuSO_4 \bullet 5H_2O$ in a solution of DMF/MeOH. A series of TEM images (Figure S8a-f) showed these Cu nanoclusters either exist either in individual form or in aggregated form. We identified the Cu nannoclusters were composed of Cu(0) via High-resolution TEM (Figure S9). A stable gel was prepared after the addition of the purified BTA-C_3-GVGVOMe into the pre-synthesized Cu clusters followed by incubation in solution

of DMF/MeOH. The formation of an ordered Cu nanoparticles array inside the oligopeptide fiber was observed in TEM images (Figure S10a and b). This observation confirmed that the ordered Cu(0) nanoparticle arrays could be formed in advance before it was organized into 1-D arrays in the presence of the peptides.

According to the plausible stacking model in Figure 4, we speculated that the oligopeptide could firstly be assembled by lateral H-bonds and grow to form rings, at the same time Cu clusters are formed during the proceeding of these rings due to the complexation of triazole groups. Here, we elaborately studied the evolution of Cu(0) 1D arrays inside the C_3-symmetric oligopeptide 3 with the gelation time (the time of the oligopeptide assembled by H-bonds to form stable gel) by controlling the gelation temperature (see Figure S7). The experimental results disclosed that there is a strong dependence of Cu(0) 1D arrays inside the C_3-symmetric oligopeptide 3 on the gelation time. If the gelation time is very fast (2 days, Figure S7a), no Cu(0) 1D arrays could be found. With the increasing of the gelation time, more and more Cu(0) 1D arrays could be seen(Figure S7b, S7c and S7d). This means that the forming of Cu clusters must be in step with the proceeding of these rings, or it is very difficult for the Cu clusters to move into the inside cavity once the oligopeptide has assembled. Furthermore, the oligopeptide could form long fibers by vertical H-bonds assembly and form a Cu clusters string (Figure 4a). Finally single fibers bunch together to form larger bundles (Figure 4b).

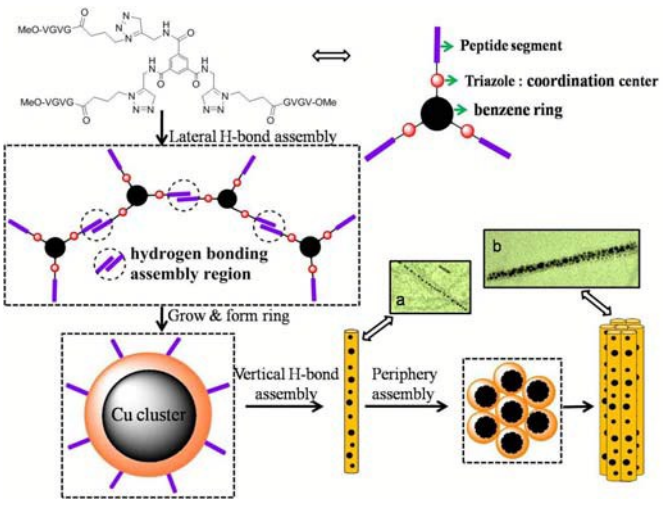

Figure 4. Plausible stacking model for One-dimensional Cu nanoclusters arrays directed by the assembly from BTA-C3-GVGVOMe.

BTA-C3-GVGVOMe might assemble into rings via β-sheet formation which provides the cavity to accommodate Cu(0) nanoparticles. Fourier transform infrared spectroscopy (shown in Figure 5) gives some evidence for the formation of β-sheet. In contrast to the FTIR spectrum of BTA-C_3-GVGVOMe&Cu powder (Figure 5a), the FTIR spectrum of the xerogel of pure BTA-C_3-GVGVOMe (Figure 5b) showed an obvious peak at 1631 cm^{-1}, which is an evidence of β-sheet formation. This indicates the incubation of the artificial oligopeptide is necessary to promote the formation of β-sheets. Although not obvious, the FTIR spectrum of the xerogel of BTA-C_3-GVGVOMe&Cu (Figure 5c) also showed a shoulder peak at 1629 cm^{-1}, which confirmed the formation of β-sheets in this organic-inorganic hybrid. The difference of the intensity of this characteristic peak might be due to the interference of the nano particles in the β-sheet formation which changed the ratio between β-sheets and other types of secondary structures of the oligopeptide. Furthermore, the oligopeptide sidechain stretching out from such rings might form H-bonding with other hexagonal or octagonal rings to form more complex nanostructures, and the stacking of such ring systems results in the formation of nanofibers with Cu(0) nanoparticles inside. The nanofibers further aggregate by forming H-bonding with each other through the oligopeptide arms stretching out from these nanofibers to pack into nanofiber bundles, so the 1D Cu nanoparticles arrays also packed into the bundles. Moreover, with the increase of Cu(0) content, the nanoparticles may also interact with triazole groups stretching out from the rings to form even larger bundles, which accounts for the topology evolution of these nanofibers when the amount of Cu(II) was increased.

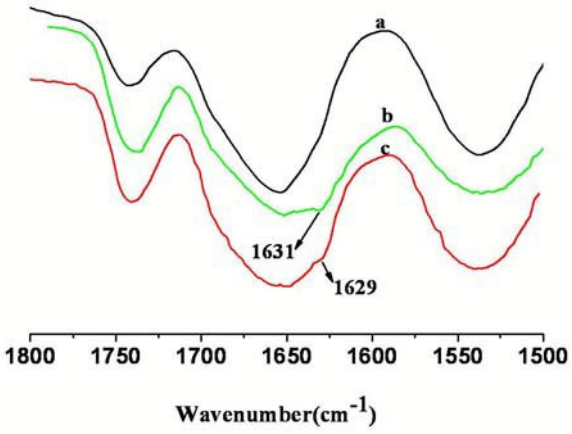

Figure 5. The amide I region of the FTIR spectra: (a) the powder of BTA-C_3-GVGVOMe &Cu, (b) xerogel of BTA-C3-GVGVOMe, (c) xerogel of BTA-C_3-GVGVOMe &Cu.

In summary, we found that by introducing coordination sites at the center of a C_3-symmetric artificial oligopeptide, Cu(0) nanoparticles 1D arrays formed inside the nanofibers composed by such oligopeptide. Different from other peptide templates with the coordination center outside which allows the growth of inorganic nanoparticles outside the nanofiber assembly, this result provides a novel concept to fabricate 1D biomaterials with inorganic elements incorporated inside, which might have potential applications such as surface-

insulated conducting nanowires. We believe that by tuning the structure of the coordination center and the structure of the self-assembly periphery, the incorporation of other metals and inorganic nanoparticles into such biomaterials could be realized. Although this assembly process occurs in organic solvent system, the extension to more environment-friendly aqueous system is also possible by structure modification. Such work is currently undergoing in our laboratory.

Acknowledgements

The authors thank the "100 Talents Program" from the Chinese Academy of Sciences, the National Natural Science Foundation of China (51403228) for financial support.

Notes and references

1 Ma, N.; Sargent, E. H.; Kelley, S. O. *J. Mater. Chem.,* 2008, 18, 954-964.

2 Gazit, E. *FEBS Journal,* 2007, 274, 317-322.

3 Dickerson, M. B.; Sandhage, K. H.; Naik, R. R. *Chem. Rev.,* 2008, 108, 4935-4978.

4 Chen, C.-L.; Rosi, N. L. *Angew. Chem. Int. Ed.,* 2010, 49, 1924-1942.

5 de la Rica, R.; Matsui, H. *Chem. Soc. Rev.,* 2010, 39, 3499-3509.

6 Banerjee, I. A.; Yu, L. T.; Matsui, H. *Proc. Nat. Acad. Sci.,* 2003, 100, 14678-14682.

7 Sharma, N.; Top, A.; Kiick, K. L.; Pochan, D. J. *Angew. Chem. Int. Ed.*, 2009, 48, 7078-7082.

8 Djalali, R.; Chen, Y.-f.; Matsui, H. *J. Am. Chem. Soc.,* 2003, 125, 5873-5879.

9 Banerjee, I. A.; Yu, L.; Shima, M.; Yoshino, T.; Takeyama, H.; Matsunaga, T.; Matsui, H. *Adv. Mater.,* 2005, 17, 1128-1131.

10 Banerjee Ipsita, A.; Yu, L.; Matsui, H. *J. Am. Chem. Soc.,* 2005, 127, 16002-16003.

11 Nuraje, N.; Su, K.; Haboosheh, A.; Samson, J.; Manning, E. P.; Yang, N. l.; Matsui, H. *Adv. Mater.,* 2006, 18, 807-811.

12 Kumara, M. T.; Tripp, B. C.; Muralidharan, S. *Chem. Mater.,* 2007, 19, 2056-2064.

13 Bai, H.; Xu, K.; Xu, Y.; Matsui, H. *Angew. Chem. Int. Ed.,* 2007, 46, 3319-3322.

14 Chen, C.-L.; Zhang, P.; Rosi, N. L. *J. Am. Chem. Soc.,* 2008, 130, 13555-13557.

15 Rehman, A.; Raza, Z. A.; Saif ur, R.; Khalid, Z. M.; Subramani C.; Rotello, V. M.; Hussain, I. *J. Colloid Interface Sci.,* 2010, 347 332-335.

16 Shi, M.; Su, W.; Matsui, H. *Nanoscale,* 2010, 2, 2373-2376.

17 Xu, H.; Wang, Y.; Ge, X.; Han, S.; Wang, S.; Zhou, P.; Shan, H., Zhao, X.; Lu, J. R. *Chem. Mater.,* 2010, 22, 5165-5173.

18 Zhang, C.; Song, C.; Fry, H. C.; Rosi, N. L. *Chemistry – A European Journal,* 2014, 20, 941-945.

19 Reches, M.; Gazit, E. *Science,* 2003, 300, 625-627.

20 Carny, O.; Shalev, D. E.; Gazit, E. *Nano Lett.,* 2006, 6, 1594 1597.

21 Ramasamy, P.; Guha, S.; Shibu, E. S.; Sreeprasad, T. S.; S S.; Banerjee, A.; Pradeep, T. *J. Mater. Chem.,* 2009, 19, 8456-8462.

22 Koley, P.; Pramanik, A. *Adv. Funct. Mater.,* 2011, 21, 4126 4136.

23 Tomizaki, K.-y.; Wakizaka, S.; Yamaguchi, Y.; Kobayashi, A.; Imai, T. *Langmuir,* 2014, 30, 846-856.

24 Gong, R. Y.; Song, Y. B.; Guo, Z. X.; Li, M.; Jiang, Y.; Wan, X. *Supramol. Chem.,* 2013, 25, 269-275.

25 Cantekin, S.; de Greef, T. F. A.; Palmans, A. R. A. *Chem. Soc. Rev.,* 2012, 41, 6125-6137.

26 Raynal, M.; Portier, F.; van Leeuwen, P. W. N. M.; Bouteill L. *J. Am. Chem. Soc.,* 2013, 135, 17687-17690.

27 Jung, S. H.; Jeon, J.; Kim, H.; Jaworski, J.; Jung, J. H. *J. Am Chem. Soc.,* 2014, 136, 6446-6452.

28 Matsuura, K.; Murasato, K.; Kimizuka, N. *J. Am. Chem. Soc* 2005, 127, 10148-10149.

29 Yang, H.; Finefrock, S. W.; Albarracin Caballero, J. D.; Wu, Y *J. Am. Chem. Soc.,* 2014, 136, 10242-10245.

30 Joy, D. C.; Joy, C. S. *Micron*, 1996, 27, 247-263.

31 Guha, P. M.; Phan, H.; Kinyon, J. S.; Brotherton, W. S.; Sreenath, K.; Simmons, J. T.; Wang, Z.; Clark, R. J.; Dalal, N. S.; Shatruk, M.; Zhu, L. *Inorg. Chem.,* 2012, 51, 3465-3477.